Mon. Not. R. Astron. Soc. **317**, 1014–1022 (2000)

The 2dF QSO Redshift Survey – I. The optical luminosity function of quasi-stellar objects

B. J. Boyle,[1] T. Shanks,[2] S. M. Croom,[3] R. J. Smith,[4] L. Miller[5] N. Loaring[5] and C. Heymans[1]

[1]*Anglo-Australian Observatory, PO Box 296, Epping, NSW 1710, Australia*
[2]*Department of Physics, University of Durham, South Road, Durham DH1 3LE*
[3]*Astrophysics Group, ICSTM, Blackett Laboratory, Prince Consort Road, London SW7 2BZ*
[4]*Research School of Astronomy and Astrophysics, ANU, Private Bag, Weston Creek PO, ACT 2611, Australia*
[5]*Department of Physics, Oxford University, 1 Keble Road, Oxford OX1 3RH*

Accepted 2000 May 24. Received 2000 May 24; in original form 1999 December 6

ABSTRACT

We present a determination of the optical luminosity function of quasi-stellar objects (QSOs) and its cosmological evolution with redshift for a sample of over 6000 QSOs identified primarily from the first observations of the 2dF QSO Redshift Survey (2QZ). For QSOs with $-26 < M_B < -23$ and $0.35 < z < 2.3$, we find that pure luminosity evolution (PLE) models provide an acceptable fit to the observed redshift dependence of the luminosity function (LF). The LF is best fitted by a two-power-law function of the form $\Phi(L_B) \propto [(L_B/L_B^*)^{\alpha} + (L_B/L_B^*)^{\beta}]^{-1}$. Exponential luminosity evolution models, both as a function of look-back time, $L_B^*(z) = L_B^*(0)\,e^{k_1\tau}$, and as a general second-order polynomial, $L_B^*(z) \propto 10^{k_1 z + k_2 z^2}$, were found to provide acceptable fits to the data set comprising the 2QZ and the Large Bright Quasar Survey. Exponential evolution with look-back time is preferred for $q_0 = 0.05$, while the polynomial evolution model is preferred for $q_0 = 0.5$. The shape and evolution of the LF at low redshifts ($z < 0.5$) and/or high luminosities, not currently well sampled by the 2QZ survey, may show departures from pure luminosity evolution, but the results presented here show that, over a significant range of redshift, PLE is a good description of QSO evolution.

Key words: methods: data analysis – surveys – galaxies: active – galaxies: fundamental parameters – quasars: general – cosmology: observations.

1 INTRODUCTION

The optical luminosity function (OLF) of quasi-stellar objects (QSOs), and its evolution with redshift, provides fundamental information on the overall demographics of the population of active galactic nuclei (AGN). It provides constraints on the physical models for QSOs (Haehnelt & Rees 1993; Terlevich & Boyle 1993), information on models of structure formation in the early Universe (Efstathiou & Rees 1988) and a picture of the ionizing ultraviolet/optical luminosity density from QSOs as a function of redshift (Meiksin & Madau 1993; Boyle & Terlevich 1998).

Based on the major ultraviolet excess (UVX) QSO surveys of the 1980s (Bracessi: Marshall et al. 1983; Palomar–Green: Green, Schmidt & Liebert 1986; Durham–AAT: Boyle et al. 1990), a picture emerged in which the low–intermediate redshift ($z < 2.2$) QSO OLF was modelled by a two-power-law function with a steep bright end [$\Phi(L_B) \propto L_B^{-3.6\pm0.1}$] and a much flatter faint end [$\Phi(L_B) \propto L_B^{-1.2\pm0.1}$] whose redshift dependence was best fitted by pure luminosity evolution (PLE), i.e., a uniform increase in luminosity towards high redshift (see e.g. Marshall 1985; Boyle, Shanks & Peterson 1988; Hartwick & Schade 1990). This evolution was modelled as a power law in redshift of the functional form $L_B^* \propto (1+z)^{k_L}$, where $3 < k_L < 3.4$ for an Einstein–de Sitter universe.

Later QSO surveys, particularly those that focused on bright magnitudes (LBQS: Hewett, Foltz & Chaffee 1993; EQS: Goldschmidt & Miller 1998; HBQS: La Franca & Cristiani 1997, 1998), have reported evidence for a more complex form of evolution in which the bright end of the OLF showed a significant steepening with increasing redshift. Indeed, the steepening was sufficiently dramatic that, at the very lowest redshifts studied, the OLF showed a single featureless power law (Koehler et al. 1997) with little evidence for any cosmic evolution amongst the brightest QSOs ($M_B < -27$). Coupled with this, further claims were made (Hawkins & Veron 1995) that the observed break in the luminosity function at higher redshifts was much less dramatic than had previously been reported.

With the increasing number of high-redshift ($z > 2$) QSOs discovered in surveys with well-defined selection criteria, evidence was also found that the strong power-law evolution does not continue on beyond $z \sim 2$. The nature of this change was modelled in a variety of ways: from a simple halt, to constant comoving density (see Boyle et al. 1991) between $z \sim 2$ and $z \sim 3$, to a slackening off of the evolution rate over the broad redshift range $1.6 < z < 3.3$ (Hewett et al. 1993; Warren, Hewett & Osmer 1994). From surveys of higher-redshift QSOs ($3.5 < z < 5.0$), strong evidence emerged for the onset of a dramatic decline in the QSO space density at $z > 3.5$ (see e.g. Warren et al. 1994).

However, compared to our knowledge of the galaxy luminosity function, QSO OLF determinations were based on relatively few objects. This was particularly true for the extremes of the redshift distribution $z < 0.3$ and $z > 4$ or the high-luminosity end of the OLF ($M_B < -27$), where departures from the pure luminosity evolution model were first noted. In these regimes, the numbers of objects in suitable surveys could be counted in the tens. Even in the most well-sampled regions of the QSO (M_B, z) plane, surveys comprised a few hundred or up to one thousand QSOs in total.

The long-heralded arrival of the new generation of large QSO surveys, compiled with facilities such as the 2dF (Lewis, Glazebrook & Taylor 1998) or Sloan Digital Sky Survey (Loveday et al. 1998), will shortly generate many tens of thousands of QSOs with which to carry out the definitive study of the QSO OLF and its evolution with redshift. These surveys also provide the opportunity to study the QSO OLF as a function of various physical parameters (e.g. emission-line strength, continuum slope) or types (e.g. BAL QSOs).

In this paper, we present a new determination of the QSO OLF based on the first ~6000 QSOs identified in the 2dF QSO Redshift Survey (2QZ) (see Smith et al. 1998). The 2QZ is currently more than a factor of 10 larger than previous QSO surveys to a similar magnitude limit ($b_J < 20.85$ mag). When complete, it is planned that the 2QZ will comprise 25 000–30 000 QSOs. In Section 2 we present a brief overview of the survey, and in Section 3 we describe the analysis of the survey. We present our conclusions in Section 4.

2 DATA

2.1 The 2dF QSO Redshift Survey

2.1.1 *Input catalogue*

For the purposes of the analysis we have used the current version (as of 1999 September) of the 2QZ catalogue containing 6684 QSOs in total. The identification of the QSO candidates for the 2QZ was based on broad-band ub_Jr colour selection from automated plate measurements (APM) of UK Schmidt Telescope (UKST) photographic plates. The survey area comprises 30 UKST fields, arranged in two $75^\circ \times 5^\circ$ declination strips centred on $\delta = -30^\circ$ and $\delta = 0^\circ$. The $\delta = -30^\circ$ strip extends from $\alpha = 21^h40$ to $\alpha = 3^h15$ and the equatorial strip from $\alpha = 9^h50$ to $\alpha = 14^h50$. The total survey area is 740 deg^2, when allowance is made for regions of sky excised around bright stars. The 2QZ area forms an exact subset of the 2dF Galaxy Redshift Survey (GRS: see Colless 1998) area, with identical 'holes' used for both surveys. In a typical 2dF field, approximately 225 fibres are devoted to galaxies, 125 to QSOs and 25–30 to sky. The data are reduced using the standard 2dF pipeline reduction system (Bailey & Glazebrook 1999).

In each UKST field, APM measurements of one b_J plate, one r plate and up to four u plates/films were used to generate a catalogue of stellar objects with $b_J < 20.85$. A sophisticated procedure was devised to ensure catalogue homogeneity (Smith 1998). Corrections were made for vignetting and field effects due to variable desensitization in the UKST plates, these effects being particularly noticeable at the edges of plates. The criteria for inclusion in the catalogue were: $(u - b_J) \leq 0.36$; $(u - b_J) < 0.12 - 0.8(b_J - r)$; $(b_J - r) < 0.05$. Based on the colours of QSOs that have previously been identified in the survey region, we estimate that the catalogue is ~90 per cent complete for $z < 2$ QSOs and comprises ~55 per cent QSOs (see Croom 1997). Subsequent spectroscopic observations with 2dF have confirmed this QSO fraction, with the principal contamination arising from Galactic subdwarfs and compact blue galaxies. Full details of the construction of the input catalogue may be found in Croom (1997) and Smith (1998).

2.1.2 *Spectroscopic observations*

2dF spectroscopic observations for the 2QZ began in 1997 January, although the bulk of the redshifts have been obtained in the observing runs after 1998 October as the 2dF system has gained functionality (increased number of fibres, faster field reconfiguration times). Over 6000 QSO redshifts have been obtained with the 2dF, and the 2QZ is now the largest single homogeneous QSO catalogue in existence. Each 2dF field in the survey is observed for typically one hour. The spectral resolution is 4 Å pixel^{-1} and the spectra cover the wavelength range 3700–8000 Å. This set-up gives a typical signal-to-noise ratio of approximately 7 or greater between 4000 and 6500 Å in the continua of the faintest objects ($b_J = 20.85$) in the 2QZ. This was sufficient to identify up to 85 per cent of the objects in each 2dF field down to this magnitude limit. Where poor conditions prevented us from achieving this identification rate in any single 2dF observation, we included in the final catalogue only those QSOs that were brighter than the magnitude at which 80 per cent of the QSO candidates in the field had a positive identification.

2.1.3 *Spectroscopic incompleteness*

In the OLF analysis below, we correct for incompleteness in the 2QZ by using an effective area that is a function of both apparent b_J magnitude and redshift. Hereinafter, all b_J magnitudes are corrected for Galactic extinction using the Schlegel, Finkbeiner & Davis (1998) values.

The 2QZ is subject to three forms of spectroscopic incompleteness. First, a small fraction of survey fields were observed in poor conditions, and do not reach the target spectroscopic completeness of 80 per cent. As described above, the magnitude limits for these fields were made brighter until the desired completeness level was reached.

Secondly, we corrected the inevitable trend to increasing spectroscopic incompleteness at fainter magnitudes by correcting the actual area observed by the fraction of objects with a reliable spectroscopic identification. This was done in 0.025-mag bins to track accurately the magnitude-dependent incompleteness.

Finally, we applied a uniform correction factor of 0.71 to the effective area to account for the 29 per cent objects in the input catalogue that have not yet been observed by 2dF, despite being located in areas already observed in the 2dF survey. This is

because the numbers of candidates in the combined QSO/galaxy catalogues in a typical 2dF field is ~50 per cent higher than the number of fibres available. Near-complete (>95 per cent) spectroscopic coverage of the survey area by 2dF is achieved by a complex tiling algorithm, with each 2dF field being visited 1.5 times on average. Since the observations are still at a relatively early stage, the coverage of the survey area with 2dF is relatively patchy and the completeness fraction is still relatively low (71 per cent). The resulting effective area of the survey is plotted in Fig. 1.

2.1.4 *Photometric incompleteness*

Photometric incompleteness, arising from the errors in the photographic magnitudes (±0.1 mag in each band) and variability (due to the non-contemporaneous nature of the ub_Jr plates on each field), will cause QSOs to exhibit $(u - b_J)/(b_J - r)$ colours outside our selection criteria. The incompleteness is a complex function of both magnitude and redshift. An estimate of this incompleteness has been made by Croom et al. (in preparation) using mean colour–redshift relations (zero-pointed to the 2QZ system) from the non-colour-selected QSO survey of Hawkins & Veron (1995). At $z < 2.3$ the Hawkins & Veron colours accurately trace the mean colours of the 2QZ QSOs. The dispersion in the colours as a function of magnitude was derived from the observed dispersion of colours for the 2QZ QSOs in the redshift interval $1 < z < 2$, the regime of highest completeness. A Monte Carlo simulation using the measured dispersion in colours and the Hawkins & Veron mean colours, with 10^6 QSOs in each Δb_J and Δz bin, was then used to predict the photometric completeness as a function of both magnitude and redshift. The completeness contours are shown in Fig. 2. The photometric completeness is largely independent of magnitude and is at least 85 per cent or greater over the redshift range $0.4 < z < 2.1$. At higher redshifts the completeness rapidly drops, falling to below 50 per cent at $z > 2.3$. We have therefore chosen this redshift as the upper limit to our analysis below. Although the catalogue contains many hundreds of QSOs with $z > 2.3$ (which will be used for the clustering analysis that is not so dependent on photometric completeness), any small errors in the completeness estimates at these redshifts can lead to large variations in the computed effective area.

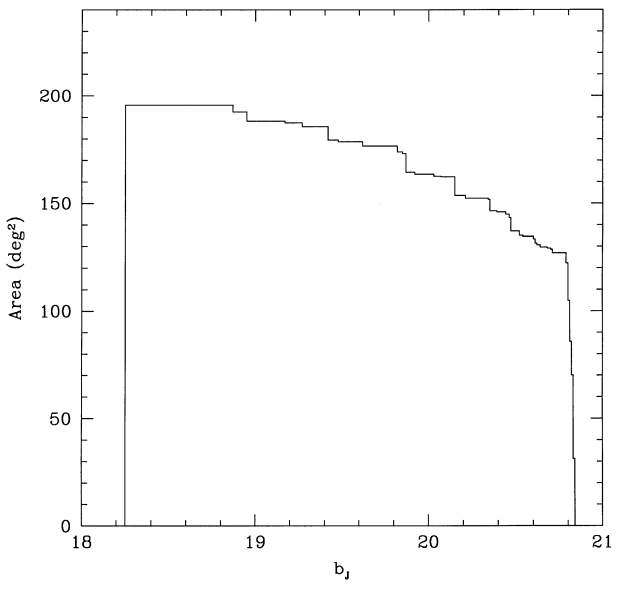

Figure 1. Coverage function for the 2dF QSO redshift survey.

At the lowest redshifts, the derived photometric completeness is still relatively high (~60 per cent at $z = 0.2$). However, low-redshift, low-luminosity QSOs ($M_B > -23$) dominated by their host galaxy light will be lost from the 2QZ as a result of the stellar selection criterion applied to the input catalogue. Although it may be possible to correct for such selection effects, for the present analysis we have simply chosen to exclude all low-luminosity QSOs ($M_B > -23$) from the OLF fitting procedure below. Given the bright apparent magnitude limit of the 2QZ ($b_J = 18.25$ mag), this effectively limits the minimum redshift in the complete 2QZ sample to $z > 0.35$. We have therefore adopted this as our low-redshift limit for all QSO surveys used in the OLF analysis below. Thus, out of a total of 6684 QSOs identified in the 2QZ (13 552 objects observed in 219 2dF fields), 5057 fulfil the criteria for inclusion in the complete sample ($q_0 = 0.5$, $H_0 = 50\,\mathrm{km\,s^{-1}\,Mpc^{-1}}$).

2.2 Other samples

We are currently in the process of extending the bright limit of the 2QZ from $b_J = 18.25$ mag to $b_J = 17$ mag using observations made with the FLAIR spectrograph on the UK Schmidt Telescope. These observations are not yet complete, and we have incorporated a number of independent QSO surveys at brighter magnitudes to extend the present analysis of the OLF to higher luminosities. Table 1 lists the areas, magnitude limits and the number of QSOs within the completeness limits ($M_B < -23$, $0.35 < z < 2.3$) for each QSO survey used in this paper. The absolute magnitudes and redshifts for the QSOs in these surveys are plotted in Fig. 3.

The Large Bright QSO Survey (LBQS: Hewett, Foltz & Chaffee 1995) provides a complementary sample to the 2QZ. The details and completeness of the survey are well established, and it provides a large number of QSOs in the 1.5–2 mag interval brighter than the $b_J > 18.25$ 2QZ survey limit.

At the brightest magnitudes $B < 16.5$ mag, the largest currently published survey is the Palomar–Green survey (Green et al. 1986). However, the completeness of this survey has been called in to question by a number of recent surveys, including the Edinburgh Quasar Survey (EQS: Goldschmidt & Miller 1998) and the Hamburg/ESO Quasar Survey (HEQS: Koehler et al. 1997). Unfortunately, full details of both these catalogues have yet to be published, and although we have access to the unpublished EQS, details of its completeness have yet to be determined accurately.

Given the remaining uncertainty over their details, and the apparent discrepancy between QSO surface densities derived from these brighter surveys, we chose to carry out our analysis of the OLF for three separate survey combinations: (a) 2QZ + LBQS; (b) 2QZ + LBQS + PG; and (c) 2QZ + LBQS + EQS + HEQS. Given the available information, the 2QZ + LBQS data sample constitutes our primary data sample in this paper. When more extensive published catalogues are available from brighter surveys (in particular the HEQS), they will clearly provide a powerful test of the OLF models at the brightest absolute magnitudes (see Fig. 3).

A further survey at intermediate magnitudes, the Homogeneous Bright QSO Survey (HBQS), is currently under construction (see Cristiani et al. 1995). There is considerable overlap between the

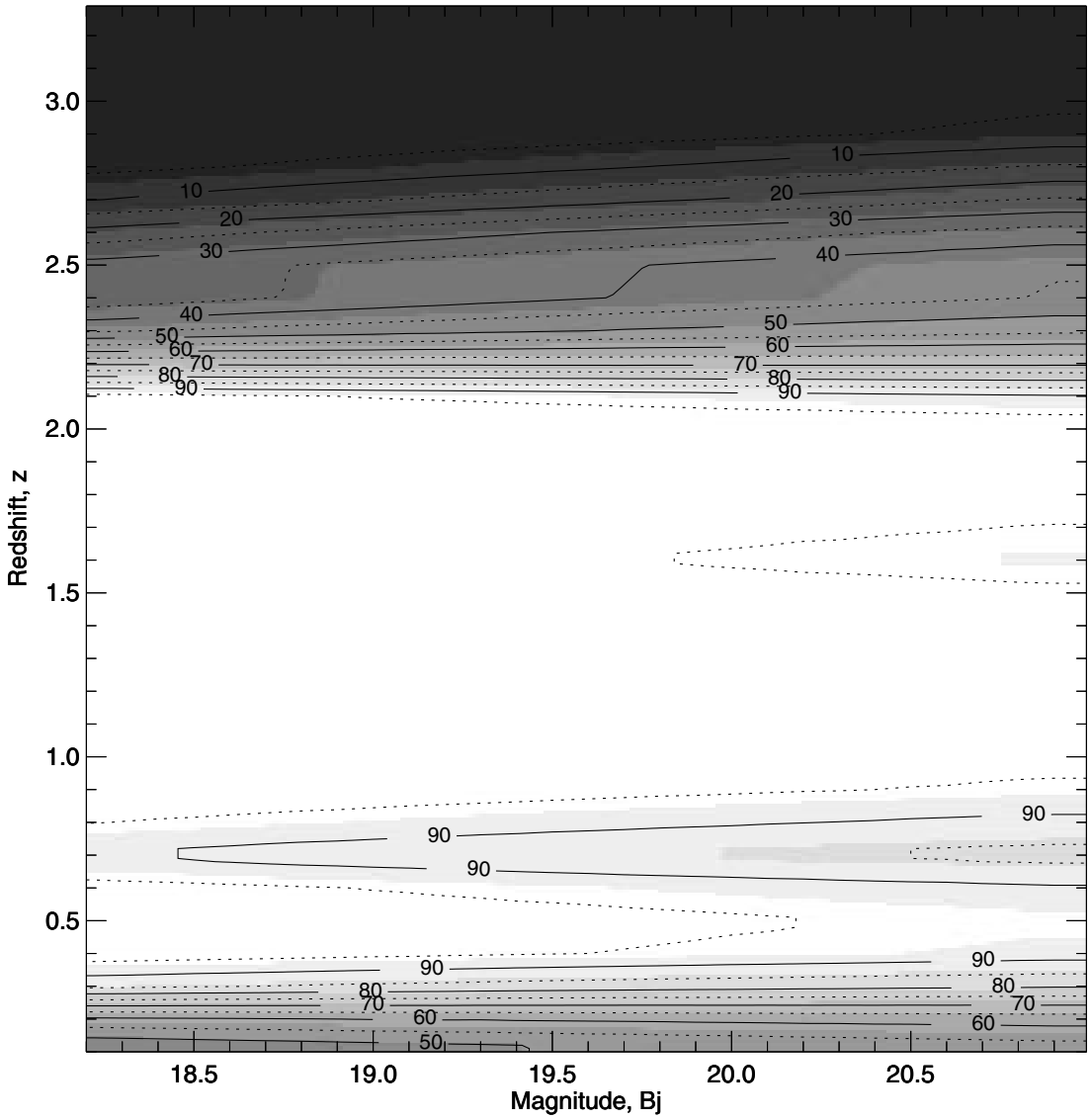

Figure 2. Photometric completeness contours in the (b_J,z) plane for the 2QZ. The contours are plotted at 5 per cent intervals: dotted lines denote 5, 15, 25, …, 95 per cent completeness; solid lines correspond to 10, 20, 30, …, 90 per cent.

survey areas for the HBQS and EQS. The currently published HBQS sample contains fewer QSOs than the EQS sample to which we have access. We have therefore chosen not to include the HBQS in the analysis below.

With one exception, the surveys are all largely independent of one another. The current coverage of the 2QZ results in a very small overlap with the LBQS; there is only one QSO in common between the 2QZ and LBQS. Given the complexity of the current 2dF coverage function in the spatial domain (due to incomplete tiling), we therefore chose to treat the LBQS and 2QZ as independent surveys. At brighter magnitudes, the PG, HEQS and EQS are all independent of one another.

The only exception is the overlap between the LBQS and EQS. There are 32 QSOs in the EQS sample that are also in the LBQS sample, or approximately 30 per cent of the EQS sample used in this analysis. The QSOs are distributed throughout the four UK Schmidt fields in common between the two surveys. In the analysis below we have therefore excluded these four fields from the EQS during the model fitting procedure, but we test the acceptability of the best-fitting model against the full EQS sample. The number of QSOs for the EQS quoted in Table 1 refers to the full sample.

3 ANALYSIS

3.1 1/*V* estimator

As the first step in our analysis, we obtained a graphical representation of the OLF and its evolution with redshift. We

Table 1. Parameters for the surveys used in our analysis. $N_{\rm QSO}$ is the number of QSOs with $M_B < -23$ ($q_0 = 0.5$, $H_0 = 50\,{\rm km\,s^{-1}\,Mpc^{-1}}$) in the redshift interval $0.35 < z < 2.3$.

Survey	$N_{\rm QSO}$	$B_{\rm lim}$	Area (deg^2)	Reference
2dF	5057	$18.25<b_J<20.85$	196	This paper
LBQS	867	$16.50<b_J<18.85$	454	Hewett et al. (1995)
EQS	106	$15.00<b_J<18.00$	330	Miller et al. (unpublished)
HEQS	23	$15.00<b_J<17.65$	611	Koehler et al. (1997)
PG	36	$13.00<b_J<16.67$	10 653	Green et al. (1986)

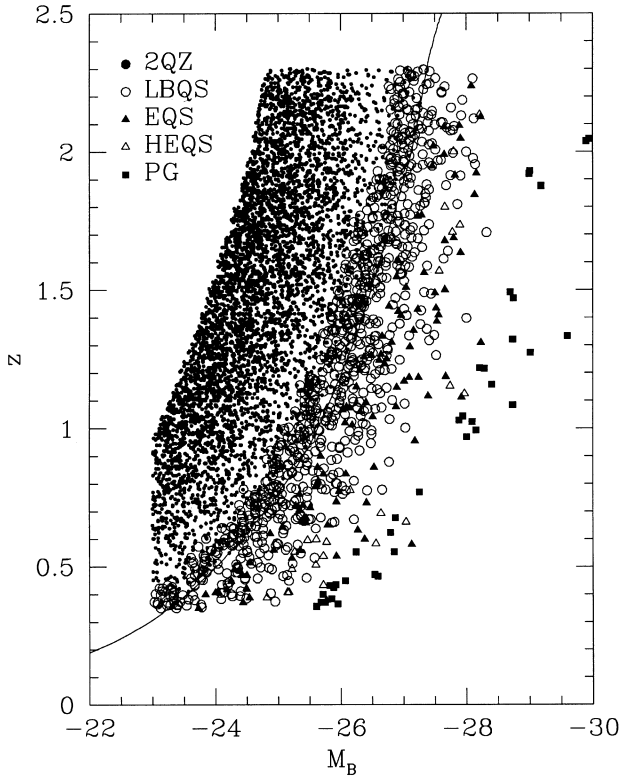

Figure 3. The (M_B,z) distribution for QSOs used in this analysis. M_B was calculated using $q_0 = 0.5$ and $H_0 = 50\,\mathrm{km\,s^{-1}\,Mpc^{-1}}$. The symbols used for the different surveys are indicated on the plot. The bright limit for the 2QZ survey, $b_J > 18.25$ mag, is denoted by the solid line.

used the new $1/V$ estimator devised by Page & Carrera (2000) to derive a binned estimate of the OLF. Although it addresses one of the potential biases of the traditional $1/V_a$ statistic (Schmidt 1968), like most binned LF estimators the Page & Carrera (2000) method assumes that absolute magnitude and redshift bins can be chosen sufficiently small so that the effects of evolution and a steeply rising OLF are negligible across each bin. For previous samples this has been difficult to achieve whilst still retaining a sufficient number of QSOs in each bin.

With the large numbers of QSOs now available for this analysis, we were able to minimize these effects by choosing much smaller bins in redshift and absolute magnitude. We used 0.25-mag bins and 10 redshift bins equally spaced in $\log(1+z)$ over the interval $0.35 < z < 2.3$ to compute the $1/V$ estimate of the OLF.

For an OLF that evolves significantly across a M_B,z bin, $1/V$ methods will still yield biased estimates of the OLF in bins cut by the magnitude limit of the sample. In such bins, the estimated OLF will only represent the mean space density of objects sampled in the bright M_B, low z region of the bin. In the absence of any magnitude limit, most objects would tend to lie in the faint M_B, high z part of the bin (at least for a power-law LF undergoing strong redshift evolution), and so the estimate of the OLF in bins that are not fully sampled will be biased low. The extent of the bias will, of course, depend on the extent to which the OLF evolves across the bin. Our choice of small bins alleviates, but does not remove, this bias, and so we have also excluded all M_B,z bins that contain the $b_J \sim 20.8$ mag survey limit in our binned estimate of the OLF. A similar bias also affects (but in the opposite sense) bins cut by the bright magnitude limit of the sample. However, we also imposed the constraint that we would not compute the OLF in bins where there were five or fewer objects. This latter condition prevents any bins cut by the bright survey limit from appearing in the estimate of the OLF below.

The resulting OLF, calculated for a flat universe with $q_0 = 0.5$ and $H_0 = 50\,\mathrm{km\,s^{-1}\,Mpc^{-1}}$, is plotted in Fig. 4. Absolute M_B magnitudes were derived for the QSOs using the k-corrections derived by Cristiani & Vio (1990). The median number of QSOs in each plotted bin is 40, although some bins contain up to 170 QSOs. The shape and redshift dependence of the OLF in Fig. 4 are strongly suggestive of a luminosity evolution model similar to those derived previously from the Durham–AAT sample (Boyle et al. 1988).

3.2 Maximum likelihood analysis

3.2.1 *Method*

To obtain a more quantitative description of suitable models, we carried out a maximum likelihood fitting procedure for a number of models to the data (see Boyle et al. 1988). This technique relies on minimizing the likelihood function S corresponding to the Poisson probability distribution function for both model and data (Marshall et al. 1983). We tested the goodness of fit of the model to the data using the 2D Kolmogorov–Smirnov (KS) statistic. The KS test is notoriously insensitive to discrepancies between the data and the model predictions in the wings of the distributions. This problem is particularly severe in the present analysis, where the weakness of the KS test at the brightest absolute magnitudes is compounded by the vanishingly small fraction of objects in this region of the M_B,z plane in the combined sample (see Fig. 3).

To alleviate this problem, we derived 2D KS statistics from each survey separately, combining them into a final KS probability using the Z statistic described by Peacock (1983). This approach enables each of the model predictions to be tested against the data in specific regions of the (M_B,z) plane sampled by different surveys. A significant rejection of the model, even by a relatively small sample, will thus have major impact on the overall acceptability of the fit.

In the fitting procedure, we used no more free parameters in any model than was required to obtain an acceptable fit. We defined a priori an acceptable fit as one that could not be rejected at the 99 per cent confidence level or greater, i.e. a KS probability (P_{KS}) of 1 per cent or greater. Errors on the fitting parameters correspond to the $\Delta S = 1$ contours around each parameter, or, equivalently, the 68 per cent confidence contour for one interesting parameter.

3.2.2 *Models*

Guided by the appearance of the OLF in Fig. 4, we chose to model the OLF $\Phi(L,z)$ as a two-power-law function in luminosity,[1]

$$\Phi(L_B, z) = \frac{\Phi(L_B^*)}{(L_B/L_B^*)^{\alpha} + (L_B/L_B^*)^{\beta}}.$$

Expressed in magnitudes, this becomes

$$\Phi(M_B, z) = \frac{\Phi(M_B^*)}{10^{0.4\{(\alpha+1)[M_B - M_B^*(z)]\}} + 10^{0.4\{(\beta+1)[M_B - M_B^*(z)]\}}},$$

where the evolution is given by the redshift dependence of the break luminosity L_B^* or magnitude $M_B^*(z)$.

We first attempted to fit the evolution by using 'standard'

[1] All simpler forms of the OLF, e.g. single power law and Schechter function, were strongly ruled out ($P_{KS} < 10^{-10}$) in preliminary fits.

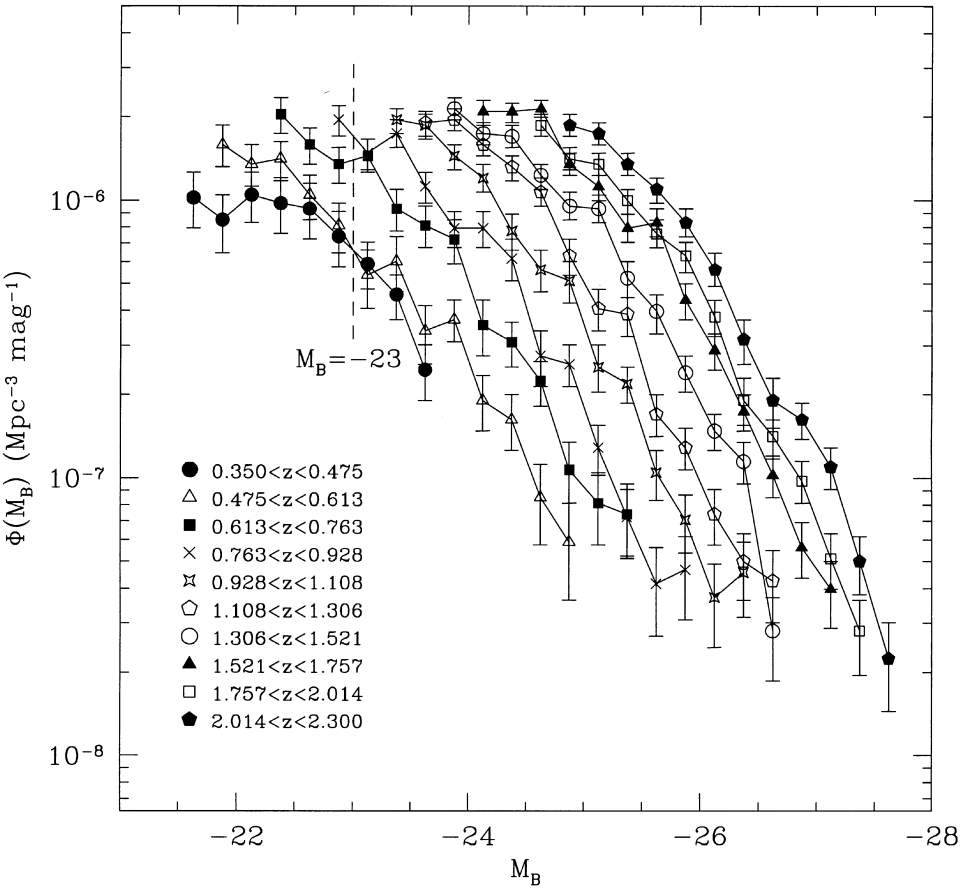

Figure 4. Luminosity function for the 2QZ + LBQS data set in a flat $q_0 = 0.5$ universe.

models, i.e. an exponential luminosity evolution with fractional look-back time (τ), such that

$$L_B^*(z) = L_B^*(0)\exp(k_1\tau),$$

and a power-law luminosity evolution model with a redshift cut-off,

$$L_B^*(z) = L_B^*(0)(1+z)^{k_1} \qquad z < z_{\max},$$

$$L_B^*(z) = L_B^*(0)(1+z_{\max})^{k_1} \qquad z \geq z_{\max}.$$

In contrast to previous analyses, the power-law evolution model provided a poor fit to all data sets ($P_{\rm KS} \ll 0.01$) for all cosmological models. This implied that any decline in the evolution at high redshifts ($z \sim 2$) was not well represented by an abrupt cut-off at $z_{\max}$. We therefore adopted a more general exponential evolution law incorporating a second-order polynomial function (hereafter referred to as 'polynomial evolution') that gives a smoother transition in the power-law behaviour of the evolution at $z > 2$ and allows for the possibility of negative evolution at high redshift:[2]

$$L_B^*(z) = L_B^*(0)10^{k_1 z + k_2 z^2},$$

or equivalently

$$M_B^*(z) = M_B^*(0) - 2.5(k_1 z + k_2 z^2).$$

3.2.3 *Results*

The best-fitting parameters, and KS probabilities for the polynomial and exponential evolution fits, are given in Table 2. The statistical errors on individual parameters are $\Delta\alpha \sim \pm 0.05$, $\Delta\beta \sim \pm 0.1$, $\Delta M_B^* \sim \pm 0.2$, Δk_1(exponential) $\sim \pm 0.1$, Δk_1 (polynomial) $\sim \pm 0.05$ and $\Delta k_2 \sim \pm 0.02$. Acceptable fits ($P_{\rm KS} > 0.01$) to the primary 2QZ + LBQS sample were found for both evolution models. The exponential model favoured low q_0 and the polynomial model favoured high q_0.

The predicted differential number–magnitude, $n(m)$, and number–redshift, $n(z)$, relations for the 2QZ survey based on the best-fitting $q_0 = 0.5$ polynomial evolution model to the 2QZ + LBQS samples are shown in Fig. 5. The model predictions provide a good fit to the derived $n(m)$ and observed $n(z)$ relations for QSOs with $0.35 < z < 2.3$ and $M_B < -23$ from the 2QZ survey also plotted in this figure.

The extrapolated maximum L_B^* in the polynomial evolution model occurs in the range $2.46 < z < 2.50$ for $0.05 < q_0 < 0.5$. The behaviour of L_B^* as a function of fractional look-back time for the $q_0 = 0.5$ universe is shown in Fig. 6.

In Fig. 7 we have also plotted the Poisson significance of the residual difference between the best-fitting $q_0 = 0.5$ polynomial

[2] Polynomial evolution models were first fitted to the radio galaxy/QSO LFs by Dunlop & Peacock (1990).

Table 2. Best-fitting OLF model parameters from maximum likelihood analysis.

Surveys sampled	Evolution model	q_0	N_{QSO}	α	β	M_B^*	k_1	k_2	Φ^* (Mpc^{-3} mag^{-1})	P_{KS}
2QZ + LBQS	$\exp(k\tau)$	0.05	6100	3.37	1.55	−21.16	7.11	–	0.47×10^{-6}	0.52×10^{-1}
	$\exp(k\tau)$	0.50	5924	3.32	1.39	−19.67	6.98	–	0.15×10^{-5}	0.14×10^{-3}
	$k_1z+k_2z^2$	0.05	6100	3.29	1.47	−22.49	1.30	−0.25	0.56×10^{-6}	0.24×10^{-2}
	$k_1z+k_2z^2$	0.50	5924	3.43	1.58	−21.99	1.35	−0.27	0.11×10^{-5}	0.12
2QZ + LBQS + PG	$\exp(k\tau)$	0.05	6136	3.37	1.63	−21.33	6.98	–	0.41×10^{-6}	0.14×10^{-1}
	$\exp(k\tau)$	0.50	5960	3.52	1.57	−20.00	6.95	–	0.10×10^{-5}	0.32×10^{-6}
	$k_1z+k_2z^2$	0.05	6136	3.30	1.55	−22.33	1.42	−0.29	0.52×10^{-6}	0.34×10^{-2}
	$k_1z+k_2z^2$	0.50	5960	3.60	1.77	−22.39	1.31	−0.25	0.68×10^{-6}	0.15×10^{-1}
2QZ + LBQS + EQS + HEQS	$\exp(k\tau)$	0.05	6265	3.95	1.87	−21.80	7.16	–	0.17×10^{-6}	0.28×10^{-1}
	$\exp(k\tau)$	0.50	6089	3.52	1.57	−20.00	6.95	–	0.10×10^{-5}	0.10×10^{-5}
	$k_1z+k_2z^2$	0.05	6265	3.39	1.47	−22.55	1.30	−0.25	0.52×10^{-6}	0.60×10^{-4}
	$k_1z+k_2z^2$	0.50	6089	3.49	1.53	−21.98	1.34	−0.27	0.61×10^{-6}	0.83×10^{-3}

evolution model and 2QZ + LBQS data set for the M_B, z bins used in the $1/V$ analysis of the OLF. It can be seen that, within the range of luminosity–redshift parameter space covered by the data, there are no significant ($>3\sigma$) differences between the model and data. Although there may be a possible weak trend at low redshifts for the model to overpredict the numbers of QSOs at low luminosities and to underpredict numbers at high luminosities, any such discrepancies are not yet statistically significant with this current data set.

We found no significant difference in the values of the best-fitting parameters when the fits were restricted to $z > 0.5$ or $z < 2.0$, i.e. excluding the sample regions where we apply the largest correction for incompleteness. The extrapolated peak in L_B^* occurs at the same redshift ($z = 2.5$) for model fits to both the $z < 2$ and $z < 2.3$ samples.

The addition of the bright samples yielded much poorer overall fits. Inclusion of the PG sample gave, at best, marginally acceptable fits for the exponential evolution model ($q_0 = 0.05$) and polynomial evolution model ($q_0 = 0.5$). No acceptable fit was found for a $q_0 = 0.5$ universe with the incorporation of HEQS and EQS, and only a barely acceptable fit ($P_{KS} = 0.01$) was obtained for the $q_0 = 0.05$ exponential evolution model.

Previous attempts to characterize departures from pure luminosity evolution (PLE) have led to models with a redshift-dependent bright-end slope (La Franca & Cristiani 1997, 1998). We attempted to fit such a model for the polynomial evolution models to the data set including the HEQS and EQS samples using a simple redshift dependence of the form

$$\alpha(z) = \alpha(0) + \kappa_3 z.$$

For $q_0 = 0.5$ the best-fitting value is $\kappa_3 = 0.36$, while for $q_0 = 0.05$ it is $\kappa_3 = 0.0$. However, this model did not provide an acceptable fit to the data set ($P_{KS} < 0.01$) for either $q_0 = 0.5$ or $q_0 = 0.05$.

By virtue of its size, rejection of the fits by the brighter data sets was dominated by the EQS. Nevertheless, the EQS contains relatively few QSOs, and a full understanding of the evolution of the very brightest QSOs clearly still requires both larger samples and a more detailed knowledge of their properties. This should be available with the completed HEQS.

There could be a variety of reasons why luminous QSOs may exhibit departures from PLE models. For example, bright QSO samples are known to contain a greater fraction of radio-loud QSOs (Peacock, Miller & Longair 1986) and also contain a greater fraction of gravitationally lensed QSOs (Kochanek 1991). Both effects could give rise to systematic departures from simple luminosity evolution models fitted predominantly to less luminous QSOs. Equally, these results may imply that luminous QSOs simply evolve differently from the bulk of 'normal' QSOs.

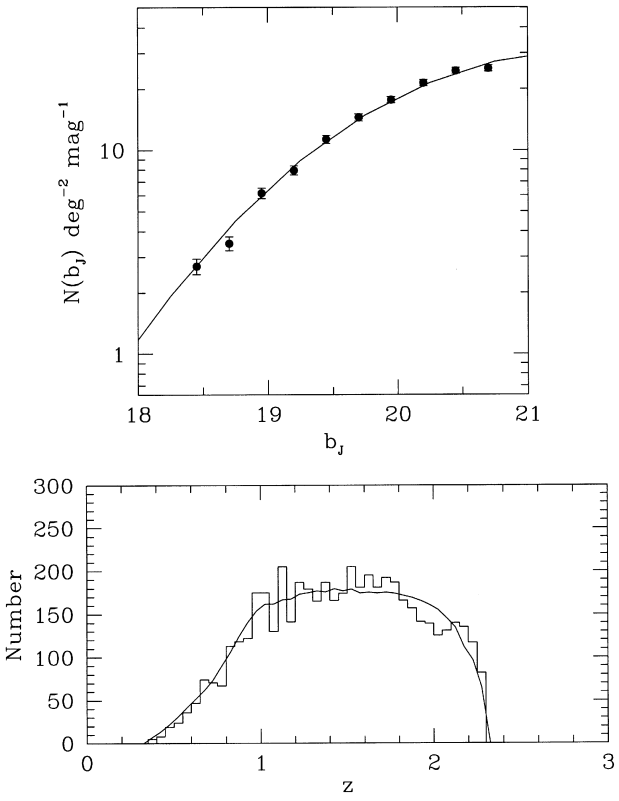

Figure 5. Upper panel: Derived differential number–magnitude, $n(m)$, relation for the 2QZ survey (filled dots) and prediction from best-fitting polynomial evolution model ($q_0 = 0.5$) to LBQS + 2QZ sample. Lower panel: Observed and predicted number–redshift, $n(z)$, relation for the 2QZ survey. Model as for upper panel. Note that the derived $n(m)$ relation from the 2QZ survey has been corrected for both spectroscopic and photometric completeness, whereas the $n(z)$ relation corresponds simply to the observed numbers of QSOs in the 2QZ survey. Correspondingly the predicted $n(m)$ relation comes directly from the model, whereas the $n(z)$ model prediction has been corrected for the assumed survey incompleteness.

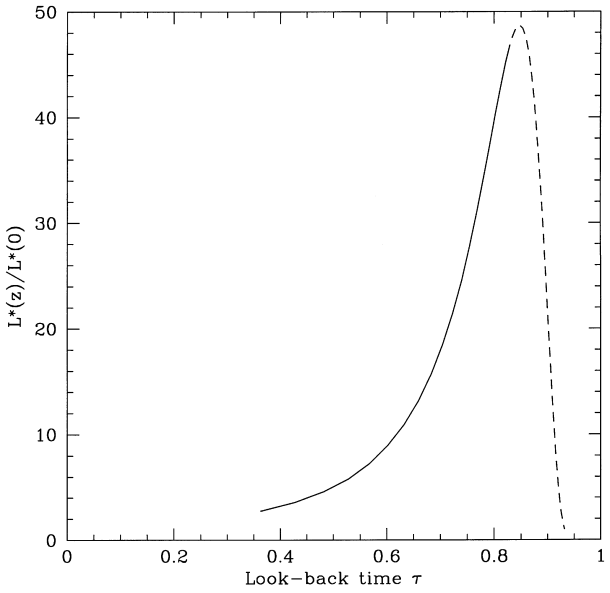

Figure 6. Evolution of L_B^* as a function of fractional look-back time (τ) for the polynomial evolution model in a $q_0 = 0.5$ universe. The solid line denotes the best-fitting evolution model obtained from fitting to the 2QZ + LBQS data sets. The dashed line represents the extrapolated evolution of L_B^* between $z = 2.3$ and $z = 5$.

We also explored the effect of different cosmological models on the OLF for our primary 2QZ + LBQS sample. The results are reported in Table 3. For an $\Omega_\Lambda = 0$ universe we fitted the polynomial evolution model to the data for a variety of different values of q_0. All values of q_0 in the range $0 < q_0 < 0.5$ yielded acceptable fits, with probability reaching a broad maximum in the region $q_0 = 0.3$–0.4. However, this value is highly dependent on the evolution model chosen to fit the data. For example, the exponential evolution model favours lower values of q_0 ($q_0 < 0.1$, see Table 2). It is unlikely that the QSO OLF can be used to define useful constraints on the value of q_0 until a meaningful physical model for QSO evolution is available.

The best-fitting OLF parameters for a non-zero cosmological constant in a flat universe (i.e. $\Omega_\mathrm{m} + \Omega_\Lambda = 1$) were also obtained using the expressions for comoving distance $r(z)$ and comoving volume element $\mathrm{d}V/\mathrm{d}z$ given by:

$$r(z) = \frac{c}{H_0 a_0} \int_0^z \frac{\mathrm{d}z}{\sqrt{\Omega_\mathrm{m}(1+z)^3 + \Omega_\Lambda}}$$

and

$$\frac{\mathrm{d}V}{\mathrm{d}z}(z) = r(z)^2 \sqrt{\Omega_\mathrm{m}(1+z)^3 + \Omega_\Lambda}.$$

A variety of fits for different values of Ω_M and Ω_Λ are presented in Table 3. Luminosity evolution remains a good fit to the 2QZ + LBQS data set in all cases. As above, it is apparent that the OLF provides little potential for discrimination between cosmological models with a non-zero Ω_Λ.

4 CONCLUSIONS

For absolute magnitudes $-26 < M_B < -23$ ($q_0 = 0.5$) and redshifts $0.35 < z < 2.3$, pure luminosity evolution (PLE) has been shown to produce an acceptable fit to the QSO distribution. This region of parameter space contains the QSOs responsible for the vast majority of the AGN luminosity density in the redshift range $0.35 < z < 2.3$. The best-fitting PLE models exhibit an exponential increase in luminosity either as a function of look-back time ($q_0 = 0.05$) or as a second-order polynomial function of redshift ($q_0 = 0.5$). In the near future, the space density of $z > 4$ QSOs predicted from extrapolations of these models may be usefully compared with the significant numbers of such QSOs now being identified at these redshifts by the Sloan Digital Sky Survey (Fan et al. 1999).

Inclusion of bright surveys, such as the EQS and HEQS, does result in departures from luminosity evolution similar in form to those seen by other authors (e.g. Hewett et al. 1993; La Franca & Cristiani 1997, 1998; Goldschmidt & Miller 1998). The principal region of parameter space in which such departures are seen lies at $z < 0.5$ where those authors claim a significant flattening of the luminosity function. The 2QZ contains relatively few QSOs with $0.35 < z < 0.5$ and does not yet probe the redshift range $z < 0.35$. Hence there is at present no inconsistency between

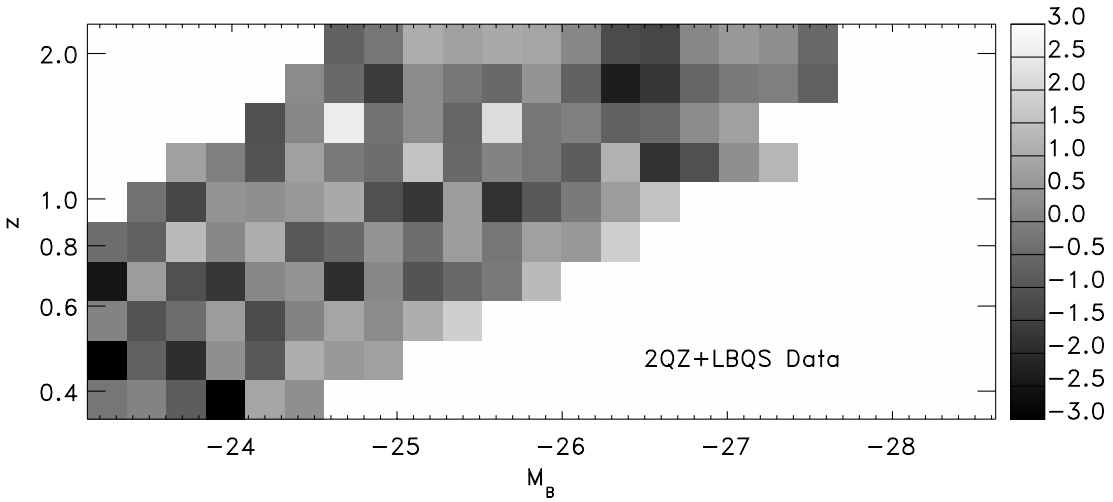

Figure 7. Grey-scale representation of the Poisson significance of the discrepancy, $(N_\mathrm{obs} - N_\mathrm{pred})/\sqrt{N_\mathrm{pred}}$, between the observed number of QSOs (N_obs) in the 2QZ + LBQS data set and predicted number of QSOs (N_pred) from the $q_0 = 0.5$ polynomial evolution model. The M_B,z bins chosen are the same as those used in the $1/V$ determination of the OLF. Only bins with $N_\mathrm{pred} > 5$ have been plotted.

Table 3. Parameter values for the polynomial evolution model as a function of Ω_m and Ω_Λ.

Ω_m	Ω_Λ	N_{QSO}	α	β	M_B^*	k_1	k_2	Φ^* (Mpc^{-3} mag^{-1})	P_{KS}
0.3	0.7	6180	3.41	1.58	−22.65	1.36	−0.27	0.36×10^{-6}	0.075
0.5	0.5	6102	3.56	1.67	−22.56	1.35	−0.27	0.44×10^{-6}	0.10
0.7	0.3	6042	3.52	1.66	−22.38	1.34	−0.26	0.51×10^{-6}	0.098
0.1	0.0	6104	3.43	1.69	−22.71	1.38	−0.28	0.35×10^{-6}	0.021
0.2	0.0	6094	3.56	1.72	−22.74	1.35	−0.27	0.36×10^{-6}	0.032
0.3	0.0	6078	3.43	1.62	−22.46	1.35	−0.27	0.54×10^{-6}	0.061
0.4	0.0	6060	3.65	1.80	−22.74	1.35	−0.26	0.36×10^{-6}	0.093
0.5	0.0	6038	3.53	1.69	−22.47	1.34	−0.26	0.56×10^{-6}	0.088
0.6	0.0	6017	3.31	1.49	−22.05	1.33	−0.26	0.10×10^{-5}	0.095
0.7	0.0	5993	3.40	1.54	−22.12	1.33	−0.26	0.94×10^{-6}	0.10
0.8	0.0	5978	3.53	1.67	−22.28	1.34	−0.26	0.76×10^{-6}	0.087
0.9	0.0	5946	3.42	1.56	−22.05	1.32	−0.26	0.11×10^{-5}	0.066
1.0	0.0	5924	3.45	1.63	−22.10	1.31	−0.26	0.10×10^{-5}	0.049

the various studies. Our analysis of the 2dF survey does, however, show that, over the redshift range $0.35 < z < 2.3$ and for absolute magnitude $M_B < -23$, PLE does provide an accurate phenomenological model of QSO evolution.

ACKNOWLEDGMENTS

The 2QZ was based on observations made with the Anglo-Australian Telescope and the UK Schmidt Telescope. We are indebted to Mike Hawkins for providing us with colour information on his QSO sample prior to publication. NL was supported by a PPARC studentship during the course of this work.

REFERENCES

Bailey J., Glazebrook K., 1999, 2dF User Manual. Anglo-Australian Observatory,
Boyle B. J., Terlevich R. J., 1998, MNRAS, 293, L49
Boyle B. J., Shanks T., Peterson B. A., 1988, MNRAS, 235, 935
Boyle B. J., Fong R., Shanks T., Peterson B. A., 1990, MNRAS, 243, 1
Boyle B. J., Jones L. R., Shanks T., Marano B., Zitelli V., Zamorani G., 1991, in Crampton D., ed., ASP Conf. Ser., Vol. 21, The Space Distribution of Quasars. Astron. Soc. Pac., San Francisco, p. 191
Colless M., 1998, in Mellier Y., Colombi S., eds, 14th IAP Meeting, Wide Field Surveys in Cosmology. Editions Frontières, Gif-sur-Yvette, p. 77
Cristiani S., Vio R., 1990, A&A, 227, 385
Cristiani S. et al., 1995, A&AS, 112, 347
Croom S. M., 1997, PhD thesis, Univ. Durham
Dunlop J. S., Peacock J. A., 1990, MNRAS, 247, 19
Efstathiou G., Rees M. J., 1988, MNRAS, 230, 5P
Fan X. et al., 1999, AJ, 118, 1
Goldschmidt P., Miller L., 1998, MNRAS, 293, 107
Green R. F., Schmidt M., Liebert J., 1986, ApJS, 61, 305
Haehnelt M. G., Rees M. J., 1993, MNRAS, 263, 168
Hartwick F. D. A., Schade D., 1990, ARA&A, 28, 437
Hawkins M. R. S., Veron P., 1995, MNRAS, 275, 1102
Hewett P. C., Foltz C. B., Chaffee F. H., 1993, ApJ, 406, L43
Hewett P. C., Foltz C. B., Chaffee F. H., 1995, AJ, 109, 1499
Kochanek C. S., 1991, ApJ, 379, 51
Koehler T., Groote D., Reimers D., Wisotzki L., 1997, A&A, 325, 502
La Franca F., Cristiani S., 1997, AJ, 113, 1517
La Franca F., Cristiani S., 1998, AJ, 115, 1688[Erratum to La Franca & Cristiani 1997]
Lewis I. J., Glazebrook K., Taylor K., 1998, in Arribas S., Mediavilla E., Watson F. G., eds, ASP Conf. Ser., Vol. 152. Astron. Soc. Pac., San Francisco, p. 71
Loveday J. et al., 1998, in Mellier Y., Colombi S., eds, 14th IAP Meeting, Wide Field Surveys in Cosmology. Editions Frontières, Gif-sur-Yvette, p. 317
Marshall H. L., 1985, ApJ, 299, 109
Marshall H. L., Tananbaum H., Avni Y., Zamorani G., 1983, ApJ, 269, 35
Meiksin A., Madau P., 1993, ApJ, 412, 34
Page M. J., Carrera F. J., 2000, MNRAS, 311, 433
Peacock J. A., 1983, MNRAS, 202, 615
Peacock J. A., Miller L., Longair M. S., 1986, MNRAS, 218, 265
Schlegel D. J., Finkbeiner D. P., Davis M., 1998, ApJ, 500, 525
Schmidt M., 1968, ApJ, 151, 393
Smith R. J., 1998, PhD thesis Univ. Cambridge,
Smith R. J., Boyle B. J., Shanks T., Croom S. M., Miller L., Read M., 1998, in McLean B. J., Golombek D. A., Hayes J. J. E., Payne H. E., eds, Proc. IAU Symp. 179, New Horizons from Multi-Wavelength Sky Surveys. Kluwer, Dordrecht p. 348
Terlevich R. J., Boyle B. J., 1993, MNRAS, 262, 491
Warren S. J., Hewett P. C., Osmer P. S., 1994, ApJ, 421, 412

This paper has been typeset from a TEX/LATEX file prepared by the author.